

# Physical and electrochemical characterization of activated carbons with high mesoporous ratio for supercapacitors based on ionic liquid as the electrolyte

Guohua Sun · Kaixi Li · Yue Liu · Jian Wang ·  
Hongwei He · Jianlong Wang · Jianyu Gu · Yanqiu Li

Received: 12 May 2010 / Revised: 9 June 2010 / Accepted: 13 June 2010 / Published online: 4 July 2010  
© Springer-Verlag 2010

**Abstract** A series of activated carbons with high mesoporous ratio were prepared by KOH reactivation based on activated carbon as the precursor. As the KOH/AC mass ratio was increased to 4:1, the mesoporous ratio increases from 60% to 76%, and the average pore size from 2.23 to 3.14 nm. Moreover, the specific capacitance for the activated carbon in ionic liquid 1-ethyl-3-methylimidazolium tetrafluoroborate ( $[EMIm]BF_4^-$ ) can reach the maximum value of  $189 \text{ Fg}^{-1}$  ( $8.0 \mu\text{Fcm}^{-2}$ ). In addition, the decrease of specific capacitance for activated carbons by KOH reactivation with current density increase shows two regimes, suggesting that activated carbons with high mesoporous ratio are much fit for charge–discharge at larger current density.

**Keywords** Activated carbon · KOH reactivation · Ionic liquid · Specific capacitance

## Introduction

Room temperature ionic liquids (RTILs) [1–5] are receiving more attention in the field of electrochemistry for their unique physicochemical properties such as high

thermal stability, relatively high ionic conductivity, wide electrochemical stability window, etc. RTILs have been applied in a variety of electrochemical devices including lithium rechargeable batteries, electric double layer capacitors (EDLCs) [6–9], and solar cells. Noticeably, it can provide higher energy density than water-system electrolytes and improve the safety and capacity retention of EDLCs at high temperatures compared to organic electrolytes. Therefore, it is considered one of the most promising electrolytes.

The energy storage mechanism in EDLCs is based on an electrostatic attraction between charges along the double layer formed at the electrode/electrolyte interface. On the basis of the mechanism, the electrode materials should have a high specific surface area for charge accumulation. However, in fact, the higher specific capacitance is not obtained from activated carbon with higher specific surface area due to the complication of activated carbon such as pore structure, functional group, pore size, etc. It has been demonstrated that the relationship between the material pore size and the ionic dimension of the solution species is especially important for the total capacitance of EDLC because of a molecular sieving effect [10–14]. Recently, template carbonization is applied to prepare mesoporous carbons with tunable structures and textures through the selection of templates, carbon precursors, etc. [15–19]. Excellent electrochemical performance of zeolite-templated carbons demonstrates the porous carbon materials should be promising candidates for electrode materials. However, the template technique is costly and requires complicated processes, which limits its industrial application.

Therefore, in the work, we have synthesized a series of activated carbons with high mesoporous ratio by KOH reactivation based on activated carbon as the precursor

G. Sun · K. Li (✉) · Y. Liu · J. Wang · H. He · J. Wang · J. Gu ·

Y. Li

Key Laboratory of Carbon Materials, Institute of Coal Chemistry,  
Chinese Academy of Sciences,  
Taiyuan, Shanxi 030001, People's Republic of China  
e-mail: likx99@yahoo.com

G. Sun · Y. Liu · H. He · J. Wang · J. Gu · Y. Li  
Graduate School, Chinese Academy of Sciences,  
Beijing 100039, People's Republic of China

**Table 1** Pore characteristics and specific capacitance of all samples with different  $R$  value

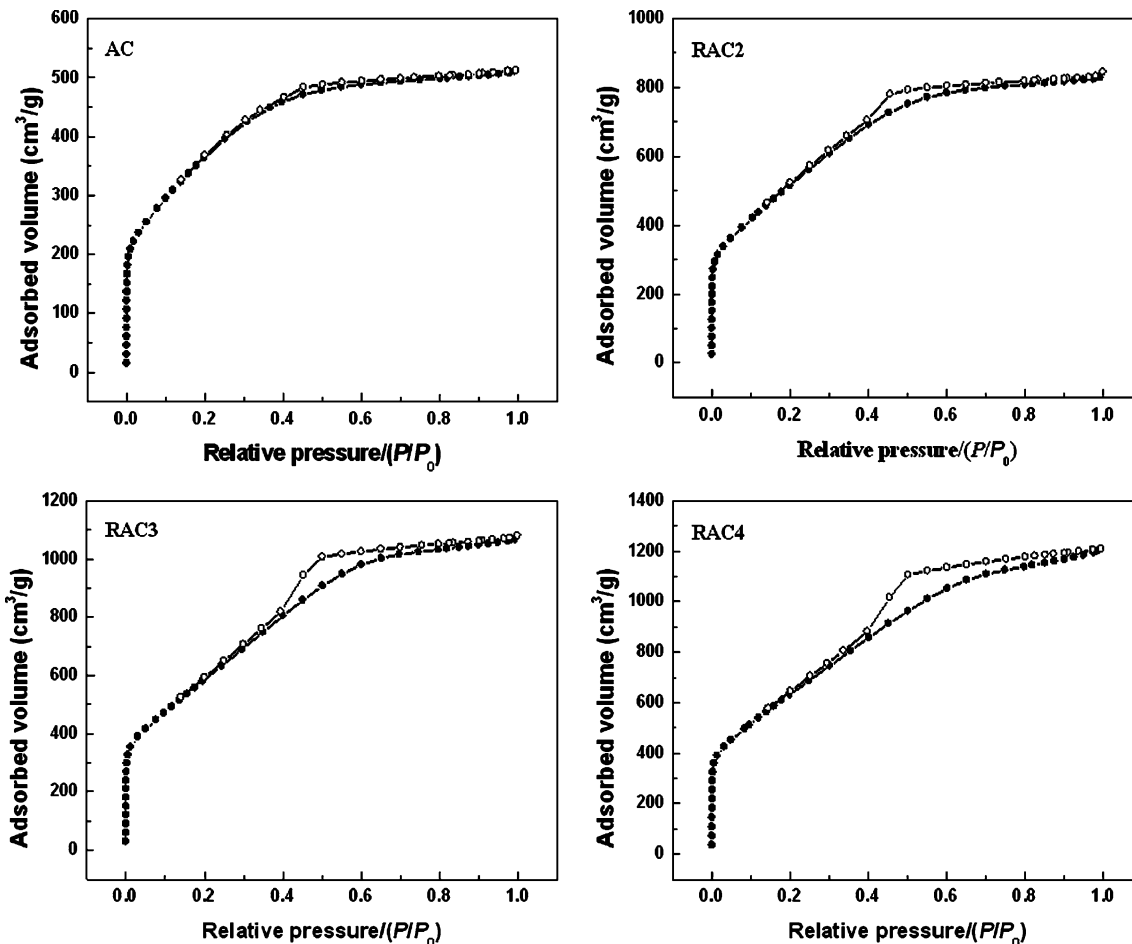
Sample	$R$ value	$S_{\text{BET}}$ ( $\text{m}^2 \text{g}^{-1}$ )	$V_{\text{total}}$ ( $\text{cm}^3 \text{g}^{-1}$ )	Ratio <sub>meso</sub> (%)	$L_0$ (nm)	Specific capacitance ( $\text{Fg}^{-1}$ )	
						Galvanostatic discharge	Impedance spectroscopy
AC	0	806	0.45	60.0	2.23	52	48
RAC2	2	1,961	1.37	68.4	2.79	150	143
RAC3	3	2,196	1.64	74.9	2.99	173	168
RAC4	4	2,357	1.85	76.0	3.14	189	183

for the purpose of enhancing specific capacitance of EDLCs. The electrochemical performance of carbon materials are tested in 1-ethyl-3-methylimidazolium tetrafluoroborate ([EMIm]BF<sub>4</sub>) at ambient temperature. The main purpose is focused not only on an advanced understanding of the electrochemical behavior of activated carbon as electrode materials for EDLCs based on ionic liquid as the electrolyte but also on the relationship between the porous structures and electrochemical performance.

## Experimental

### Synthesis of [EMIm]BF<sub>4</sub>

To prepare 1-ethyl-3-methylimidazolium bromide ([EMIm]Br), the precursor for [EMIm]BF<sub>4</sub>, 90 cm<sup>3</sup> ethylbromide (Chemistry Reagent Co. Ltd of Shanghai, China H<sub>2</sub>O<0.005%) was first slowly added to a solution of 35 cm<sup>3</sup> of 1-methylimidazole (Michael Kors H<sub>2</sub>O<0.005%) in 100 cm<sup>3</sup> of 1,1,1-trichloroethane under stirring conditions.

**Fig. 1** Nitrogen adsorption–desorption isotherms of all samples

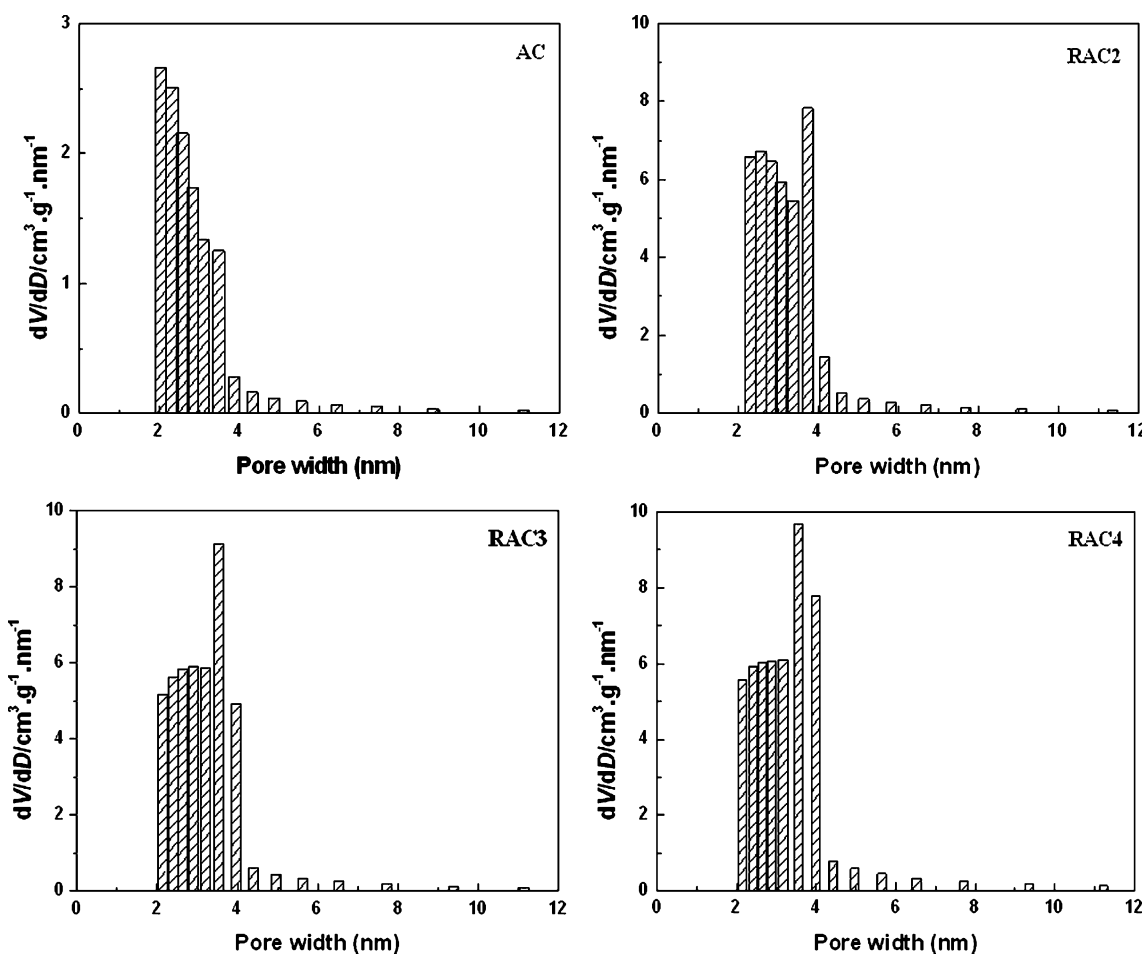


**Fig. 2** Pore size distribution of all samples

The mixture was further stirred for 3 h at ambient temperature before reflux at 70 °C for 24 h. The mixture was then allowed to cool completely and age for about 12 h, thus giving rise to the formation of a two-phase system. After separation from the mixture using a separatory funnel, the lower phase containing [EMIm]Br was washed twice with 100 cm<sup>3</sup> portions of 1,1,1-trichloroethane and then dried at 70 °C under reduced pressure. The yield of [EMIm]Br is 69.3 g (57.6 wt.%).

Next, 10.5 g of NH<sub>4</sub>BF<sub>4</sub> was added into 250 cm<sup>3</sup> acetonitrile (Chemistry Reagent Co. Ltd of Shanghai, China H<sub>2</sub>O<0.005%) containing 19.2 g [EMIm]Br, and the solution was stirred for 6 h. The white NH<sub>4</sub>Br precipitate was filtered off, and acetonitrile was evaporated from the clear filtrate at 60 °C under vacuum; the remaining liquid salt, [EMIm]BF<sub>4</sub>, was dried for 12 h at 80 °C under vacuum. The yield of [EMIm]BF<sub>4</sub> is 12.5 g (78.2 wt.%).

#### Preparation of activated carbons with high mesoporous ratio

The preparation of activated carbons with high mesoporous ratio was carried out by means of KOH reactivation for

which activated carbon (commercial purchase from Xinhua Co. Ltd of Shanxi, China) was chosen as precursor. A solution of activated carbon, KOH and H<sub>2</sub>O ( $m_{AC}:m_{KOH}=2-4$ ) was well agitated and dispersed by ultrasonic. After stabilized in air for 12 h at ambient temperature, the mixture was heated at a rate of 4 °C min<sup>-1</sup> to 850 °C and maintained at this temperature for 1 h in N<sub>2</sub>. The resultant samples were washed with deionized water to neutral and then dried at 105 °C for 12 h. The initial activated carbon and reactivated carbons based on different KOH/AC mass ratio ( $R$  value) were denoted as AC, RAC2, RAC3, and RAC4, respectively. The main parameters of all samples were shown in Table 1.

Specific surface area and pore structure were characterized by N<sub>2</sub> adsorption-desorption isotherms at 77 K (Sorptomatic 1990, Italy). The specific surface area was obtained using Brunauer–Emmett–Teller (BET) method. Pore size distribution was calculated from the desorption branch of the nitrogen isotherm using Bopp–Jancso–Heinzinger (BJH) method. The total pore volume ( $V_{total}$ ) was calculated at the relative pressure of 0.99. Average pore size ( $L_0$ ) was obtained using BJH method.

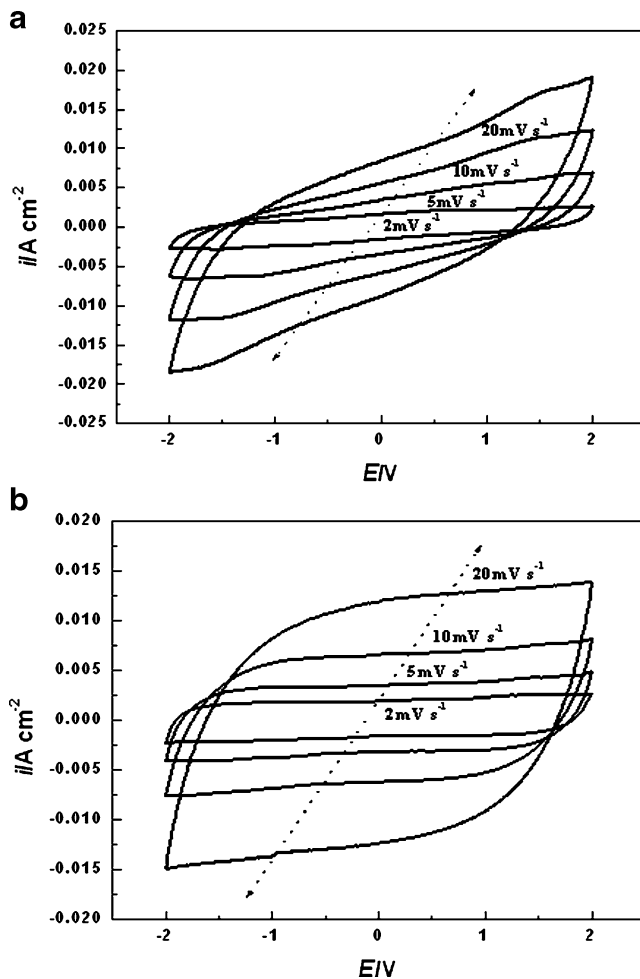


**Fig. 3** Cyclic voltammograms of **a** AC and **b** RAC4 based on [EMIm]BF<sub>4</sub> as the electrolyte

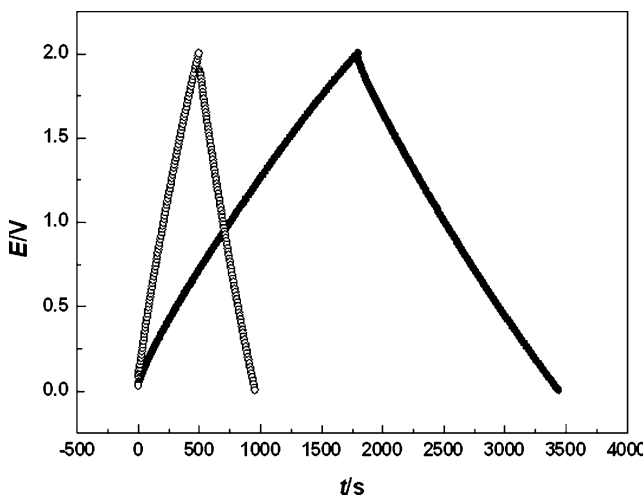


**Fig. 4** Galvanostatic charge-discharge curves of AC (circle) and RAC4 (filled circle) based on [EMIm]BF<sub>4</sub> as the electrolyte

## Preparation of electrodes and capacitors

RACs (85 wt.%), graphite (10 wt.%), and polytetrafluoroethylene (5 wt.%) were mixed and stirred adequately, and the paste thus formed was pressed onto a foam nickel. The electrodes formed in this way were 10 mm in diameter and 0.2 mm in thickness. The charge collector (stainless steel), electrode, separator (polypropylene)/electrolyte solution, electrode, and charge collector were assembled in sequence as a sandwich and enveloped in a cell.

## Measurement of electrochemistry performance

Electrochemical performance was measured by using Arbin BT-4+ (America). Based on galvanostatic charge-discharge experiments, the  $C$  (F g<sup>-1</sup>) of a single electrode was calculated from the formula  $C = 2It/\Delta Vm$ , where  $I$  was the discharge current,  $t$  was the discharge time,  $\Delta V$  was the potential change in the discharge, and  $m$  was the mass of the active electrode material. Impedance measurements were performed at the electrochemistry station (CHI600C) at open circuit voltage with a ±5 mV voltage amplitude and wide frequency range (100 kHz–10 mHz). The capacitors were cycled between 0 and 2 V in [EMIm]BF<sub>4</sub> for maintaining steady electrochemical performance.

## Results and discussion

The N<sub>2</sub> adsorption–desorption isotherms at 77 K for AC and RACs are presented in Fig. 1. The isotherm is typical type-I for AC with well-defined plateaus, indicating the apparent micropore characteristic of the carbon material. However, type-IV isotherms could be found for RACs. It is clear that RACs exhibit hysteresis loops over a wide range of relative

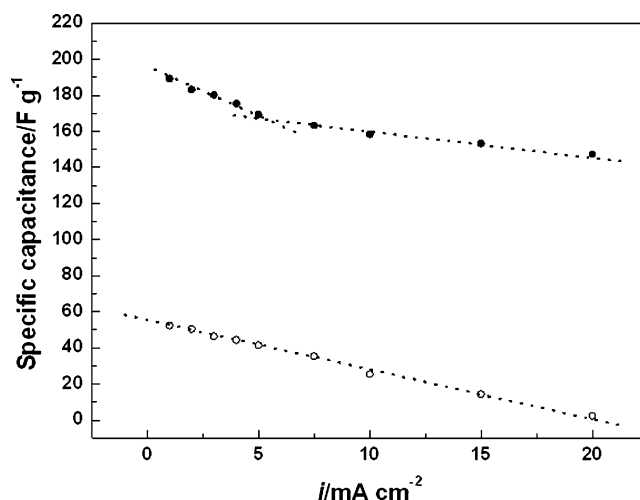


**Fig. 5** Specific capacitance versus current density for AC (circle) and RAC4 (filled circle)

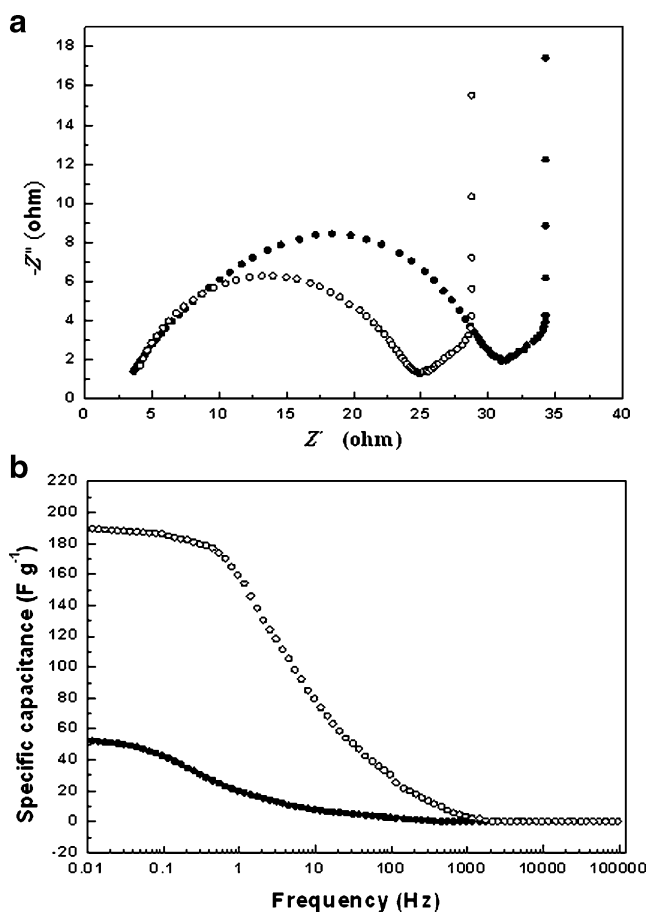


**Fig. 6** **a** Niquist plots and capacitance versus **b** frequency dependence of AC (filled circle) and RAC4 (circle) based on [EMIm]BF<sub>4</sub> as the electrolyte

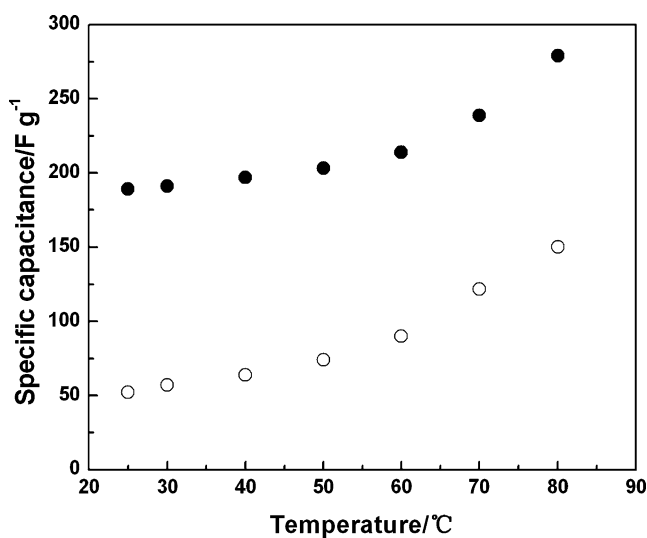


**Fig. 7** Specific capacitance versus temperature for AC (circle) and RAC4 (filled circle)

pressure (0.4~0.9), which is associated with the capillary condensations taking place in the mesopores [20], suggesting that some mesopores occur clearly for RACs. Furthermore, the hysteresis loops for RACs are more obvious with  $R$  value increase, indicating the mesoporous ratio of carbon materials increases with the amount of KOH increase.

Figure 2 presents pore size distribution of AC and RACs, respectively. The peaks at 3.53 and 4 nm point out that the pores of 3.53 and 4 nm are developed abundantly for RACs. Moreover, the bigger the  $R$  value, the more abundant pores with 3.53 and 4 nm are. The explanation is that metal potassium can intercalate easily into micropores of activated carbon and further etch the micropore structures to develop the mesopores at high temperature [21–25].

The porous texture parameters of all samples are listed in Table 1. Both the BET surface area and total pore volume increase dramatically with the  $R$  value and reach the maximum value of  $2,357 \text{ m}^2 \text{ g}^{-1}$  and  $1.85 \text{ cm}^3 \text{ g}^{-1}$ , respectively, at  $R=4$ , a highly developed porous structure. The mesoporous ratio and average pore size of carbon materials increase markedly with the increase of the  $R$  value and reach the maximum value 76% and 3.14 nm for RAC4. The RAC samples with  $R$  value over 2 possess both high surface area and well-developed mesoporous structure, which is very attractive for EDLCs.

For simplicity, sample RAC4 is adopted for comparison of electrochemical performance with AC based on [EMIm]BF<sub>4</sub> as the electrolyte. Figure 3 shows cyclic voltammograms of AC and RAC4 in [EMIm]BF<sub>4</sub> at voltage scan rates of 2, 5, 10, and 20 mV s<sup>-1</sup>. The well-defined rectangular voltammograms without any peaks for two

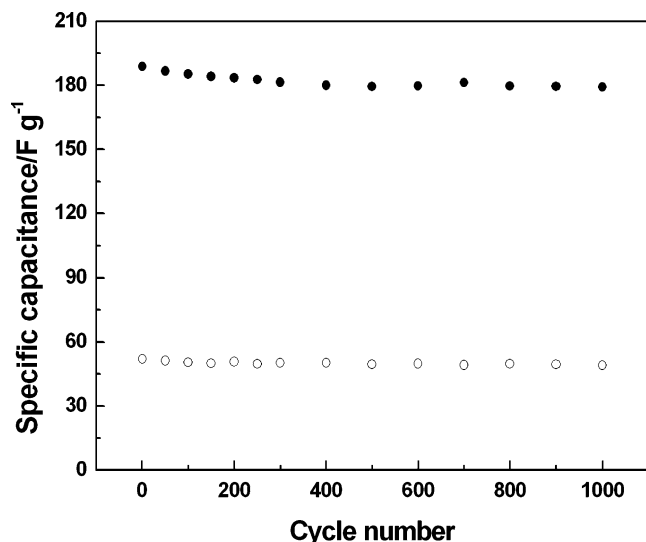


**Fig. 8** Cycle life of EDLCs based on AC (circle) and RAC4 (filled circle) as electrode materials at a constant current density of  $1 \text{ mA cm}^{-2}$

samples at the low voltage sweep rate of  $2 \text{ mVs}^{-1}$  suggest a pure electrostatic attraction, i.e., a typical capacitive behavior. But these become distorted with the increase of voltage scan rate, especially that of AC in  $[\text{EMIm}] \text{BF}_4$ , which are considered to be usually associated with ohmic loss of EDLCs due to large interface impedance resulting from narrow micropores of carbon material.

Galvanostatic charge–discharge is performed to determine specific capacitance of AC and RAC4. The linear voltage–time dependence for AC and RAC4 demonstrates the typical capacitive behavior of the cell (Fig. 4). The specific capacitance of AC and RAC4 is found to be 52 and  $189 \text{ Fg}^{-1}$  ( $6.4 \text{ and } 8.0 \mu\text{Fcm}^{-2}$ ), respectively, at  $1 \text{ mA cm}^{-2}$ . The specific capacitance value of other samples is shown in Table 1. The specific capacitance for AC is almost consistent with literature data reported, but for RAC4 is high than corresponding data [26], suggesting important influence of mesopores on specific capacitance.

Variation in the specific capacitance versus current density for AC and RAC4 is shown in Fig. 5. As the current density increases, the specific capacitance decreases, but behavior occurred in a different manner for two samples. The specific capacitance almost decreases linearly for AC as the current density increases. However, the curve of specific capacitance versus current density for RAC4 shows two regimes. The specific capacitance decreases sharply as the current density increases at a small current density range, but a slow decrease of the specific capacitance can be observed as current density increase, which may be associated to the presence of mesopores [27]. The experimental results show that RACs are much fit for charge–discharge at larger current density.

Electrochemical impedance spectroscopy (EIS) has been used to investigate the performance of EDLCs such as internal resistance, capacity, etc. Fig. 6a shows the relation between  $Z''$  (imaginary) and  $Z'$  (real) impedance components of EDLCs based on AC and RAC4 as the electrode materials, respectively. The Niquist plots of AC and RAC4 consist of a semicircle at high frequency, a line with a slope close to  $45^\circ$  within the middle frequency, and an almost vertical line at low frequency. However, the Niquist plot of AC has a large semicircle at high frequency; it can be suggested that there is large resistance at the interface of electrode/electrolyte due to small pore structure of activated carbon compared to ion dimension, which will result in the serious deterioration of the capacitance at high discharge current. The capacitance–frequency dependence of EDLCs based on AC and RAC4 as the electrode materials is shown in Fig. 6b. The specific capacitance of AC and RAC4 is calculated using the following formula:

$$C = \frac{-1}{2\pi f \times Z_{\text{im}}} \quad (1)$$

where  $f$  is the applied frequency;  $Z_{\text{im}}$  is the imaginary part of impedance. The capacitance values of AC and RAC4 measured by EIS are lower than that measured by galvanostatic charge–discharge due to the fact that alternating current penetrates into the electrode bulk with more hindrance [28].

Figure 7 shows specific capacitance versus temperature for AC and RAC4. The specific capacitance for two samples increases gradually, as the temperature increases, and reaches the maximum value of 150 and  $279 \text{ Fg}^{-1}$ , respectively, at  $80^\circ\text{C}$ . This can be ascribed to viscosity decrease and conductivity increase of ionic liquid due to increasing temperature.

The long cycle stability of EDLCs based on AC and RAC4 as the electrode materials in  $[\text{EMIm}] \text{BF}_4$  during galvanostatic charge–discharge processes is also measured (shown in Fig. 8). After 1,000 cycles, only about 5.8% for AC and 5.1% for RAC4 loss of capacitance can be found.

## Conclusion

Pore structures of activated carbon can remarkably change by KOH reactivation. When the KOH/AC mass ratio is 4, the mesoporous ratio and average pore size reach the maximum value of 76% and 3.14 nm, respectively. Moreover, a high specific capacitance of  $189 \text{ Fg}^{-1}$  ( $8.0 \mu\text{Fcm}^{-2}$ ) based on ionic liquid as the electrolyte for RAC4 can be obtained. The results indicate that activated carbons with high mesoporous ratio prepared by KOH reactivation are promising electrode materials for EDLC.

**Acknowledgment** This work was financially supported by National Nature Science Foundation of China (No. 50272070) and Shanxi Province Science Foundation for Youths (No. 2010021023-3).

## References

1. Akihiro N, Kikuko H, Masayoshi W (2001) J Phys Chem B 105:4603
2. Rika H, Takayuki H, Tetsuya T, Yasuhiko I (2002) J Electrochem Soc 149:D1
3. Maciej G, Andrzej L, Izabela S (2006) Electrochim Acta 51:5567
4. Andrea B, Ugo B, Stefano C, Mastragostino M, Francesca S (2004) Electrochim Commun 6:566
5. Mariachiara L, Marina M, Francesca S (2007) Electrochim Commun 9:1567
6. Wu FC, Tseng RL, Hu CC, Wang CC (2005) J Power Sources 144:302
7. Hsieh CT, Lin YT (2006) Microporous Mesoporous Mater 93:232
8. Lewandowski A, Świderska A (2003) Solid State Ionics 161:243
9. Liu HT, Zhu GY (2007) J Power Sources 171:1054
10. Salitra G, Soffer A, Eliad L, Cohen Y, Aurbach D (2000) J Electrochem Soc 147:2486
11. Eliad L, Salitra G, Soffer A, Aurbach D (2001) J Phys Chem B 105:6880

12. Eliad L, Salitra G, Soffer A, Aurbach D (2002) *J Phys Chem B* 106:10128
13. Raymundo-Piñero E, Kierzek K, Machnikowski J, Béguin F (2006) *Carbon* 44:2498
14. Yansu W, Chengyang W, Chunyu G, Zhiqiang S (2008) *J Phys Chem Solids* 69:16
15. Zhibin L, Lizhen A, Liqin D, Mingyi Z, Jingying S, Shiying B, Yindi C (2009) *Microporous Mesoporous Mater* 119:30
16. Campesi R, Cuevas F, Leroy E, Hirscher M, Gadiou R, Vix-Guterl C, Latroche M (2009) *Microporous Mesoporous Mater* 117:511
17. Darmstadt H, Roy C, Kaliaguine S, Joo SH, Ryoo R (2003) *Microporous Mesoporous Mater* 60:139
18. Xu DP, Yoon SH, Mochida I, Qiao WM, Wang YG, Ling LC (2008) *Microporous Mesoporous Mater* 115:461
19. Zhihong T, Yan S, Yongming T, Lang L, Quangui G (2008) *Microporous Mesoporous Mater* 111:48
20. Huanlei W, Qiuming G, Juan H (2009) *J Am Chem Soc* 131:7016
21. Qiao WM, Yoon SH, Mochida I (2006) *Energy Fuels* 20:1680
22. Lillo-Ródenas MA, Lozano-Castelló D, Cazorla-Amorós D, Linares-Solano A (2001) *Carbon* 39:751
23. Marsh H, Yan DS, O'Grady TM, Wennerberg A (1984) *Carbon* 22:603
24. Lillo-Ródenas MA, Cazorla-Amorós D, Linares-Solano A (2003) *Carbon* 41:267
25. Yoon SH, Lim SY, Song Y, Qiao WM, Tanaka A, Mochida I (2004) *Carbon* 42:1723
26. Lewandowski A, Galiński M (2004) *J Phys Chem Solids* 65:281
27. Fuertes AB, Fernando P, Jose MR (2004) *J Power Sources* 133:329
28. Xing W, Qiao SZ, Ding RG, Li F, Lu GQ, Yan ZF, Cheng HM (2006) *Carbon* 44:216